Supplemental Information

Visible-light responsive S-vacancy $ZnIn_2S_4$/N-doped TiO_2 Nanoarrays Heterojunction for high-performance photoelectrochemical water splitting

Zhiyong Bao[a], Yu Jiang[a], Zhihong Zhang[a], Jun Lv[a]*, Wangqiang Shen[a], Jiyan Dai[b]*, Jiaheng Wang[a], Jing Cai[a], Yucheng Wu[a]*

[a] School of Materials Science and Engineering and Anhui Provincial Key Laboratory of Advanced Functional Materials and Devices, Hefei University of Technology, Hefei 230009, China

E-mail: lvjun117@126.com; ycwu@hfut.edu.cn

[b] Department of Applied Physics, The Hong Kong Polytechnic University, Hong Kong.

E-mail: jiyan.dai@polyu.edu.hk

Figure S1 The XRD patterns of N-TZ-0.1.
Figure S2 SEM images of (a-b)TiO_2, (c-d)N-TiO_2 and (e-f) Sv-ZIS
Figure S3 SEM images of (a-b) N-TZ-0.01, (c-d)N-TZ-0.05 and (e-f)N-TZ-0.1
Figure S4 Photoelectrochemical water splitting video of heterostructure photocatalyst
Figure S5 Photocatalytic H_2/O_2 evolution performance of N-TZ-0.025
Figure S6 LSV curves of all samples under light (a) and dark (b) conditions, (c) photocurrent response, (d) electrochemical impedance spectroscopy (EIS) of all samples
Figure S7 UV-vis absorption spectra of Sv-ZIS
Figure S8 Measured IPCE in the visible-light range
Table S1 The representative research results of TiO_2-based heterojunction and homojunction

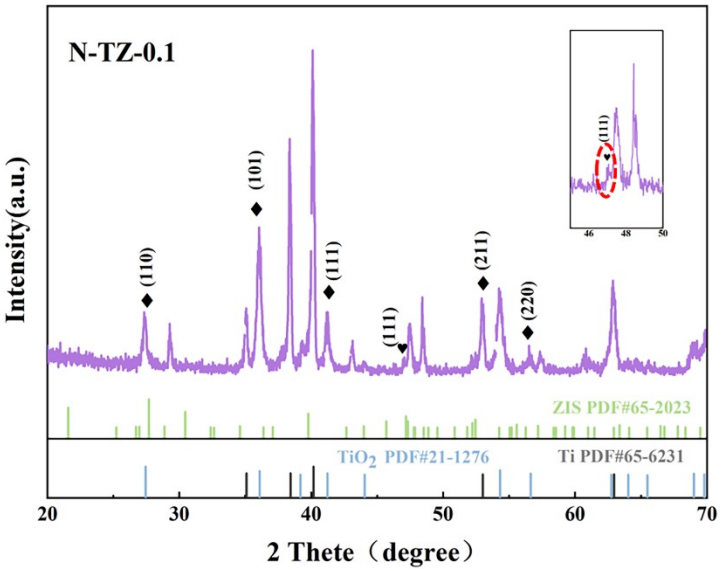

Figure S1. The XRD pattern of N-TZ-0.1.

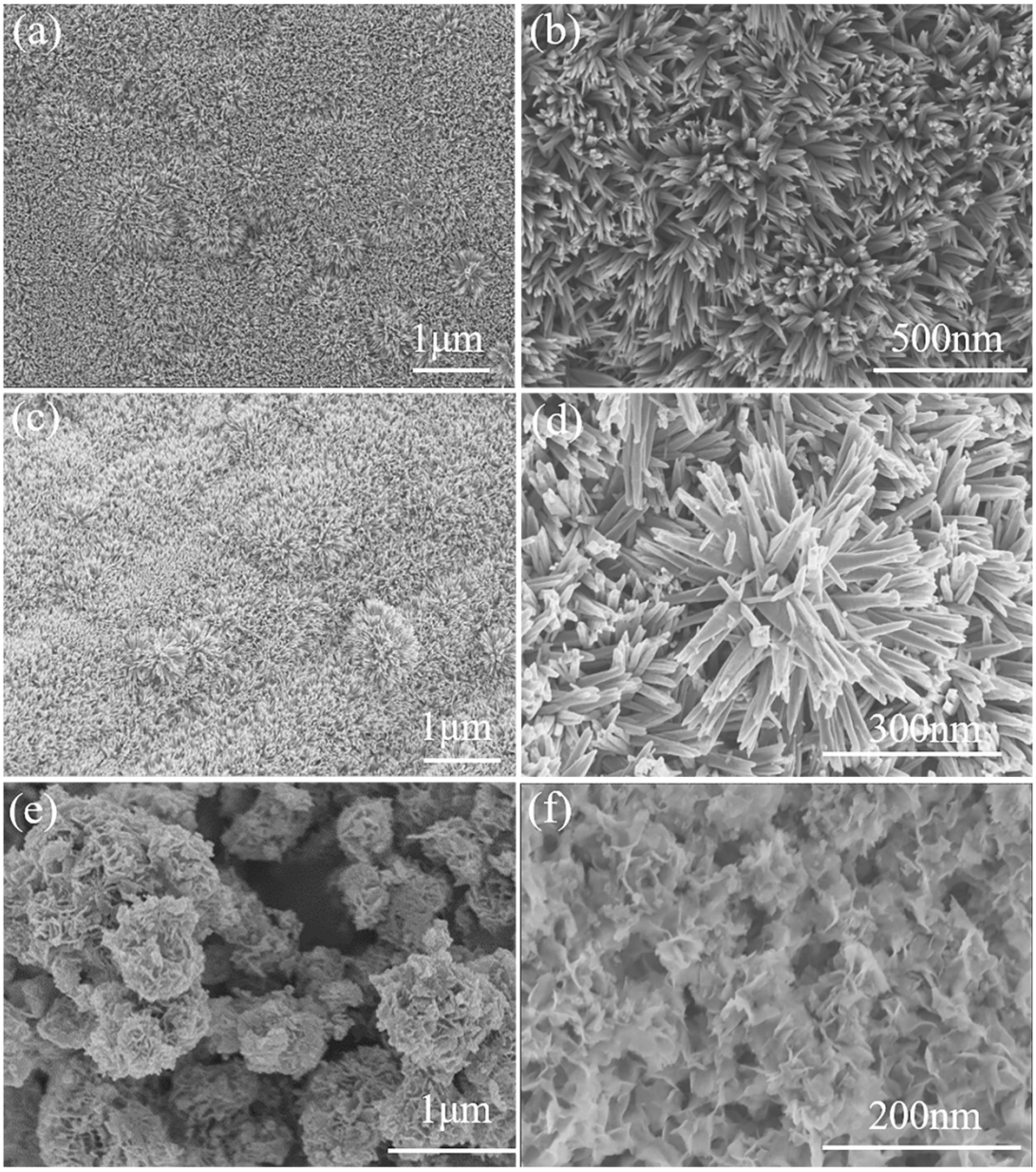

Figure S2 SEM images of (a-b)TiO_2, (c-d)N-TiO_2 and (e-f) S_v-ZIS

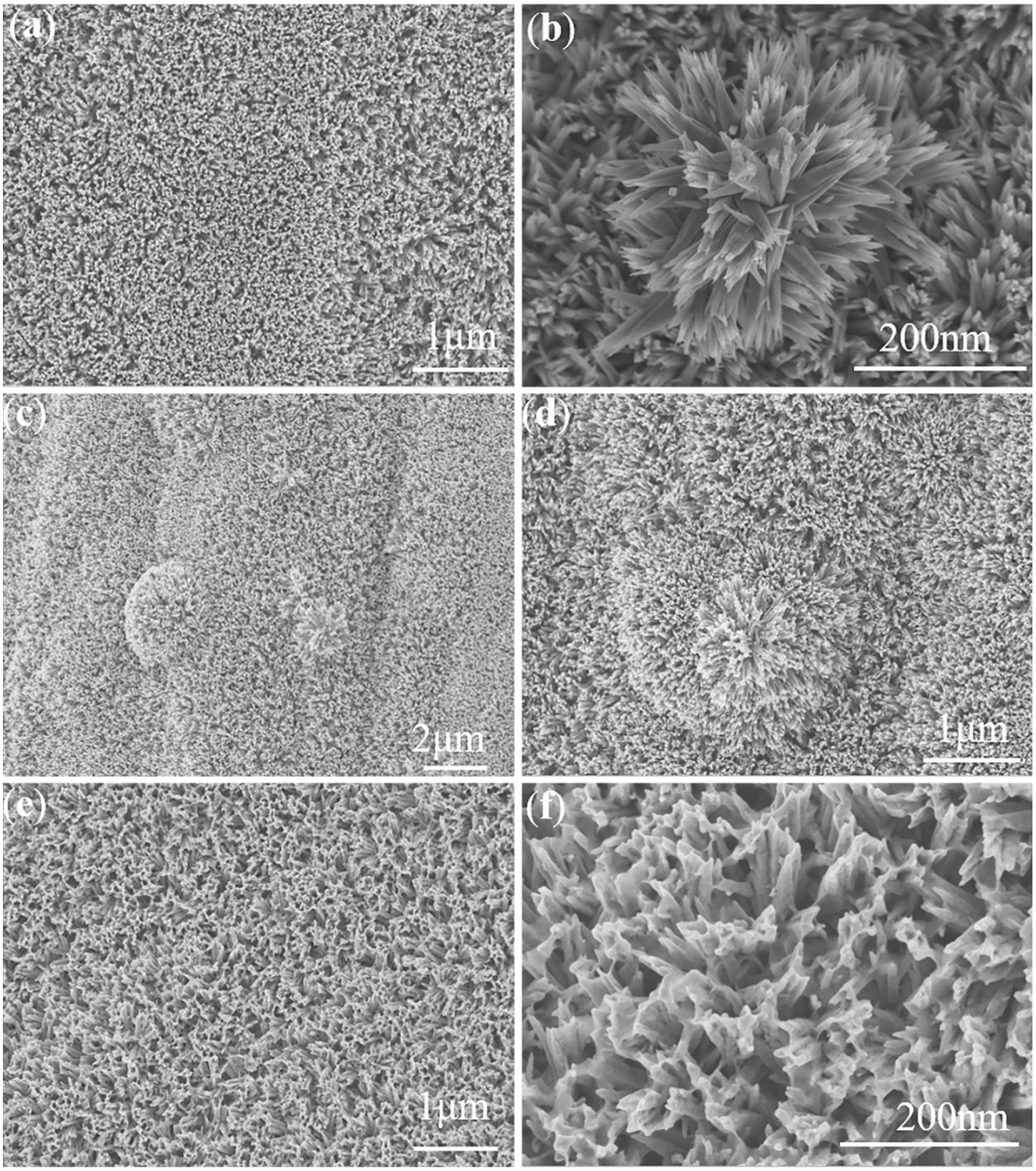

Figure S3 SEM images of (a-b) N-TZ-0.01, (c-d)N-TZ-0.05 and (e-f)N-TZ-0.1

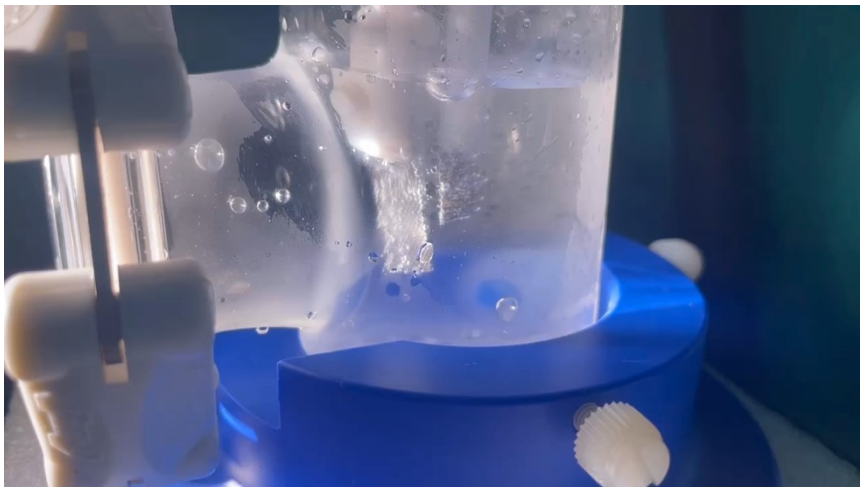

Figure S4 Photoelectrochemical water splitting video of heterostructure photocatalyst

In this video, you can see that a large number of bubbles produced by both the photocathode and the photoirradiated photoanode, especially the number of hydrogen bubbles produced by the photocathode is higher than oxygen bubbles produced by the photoanode.

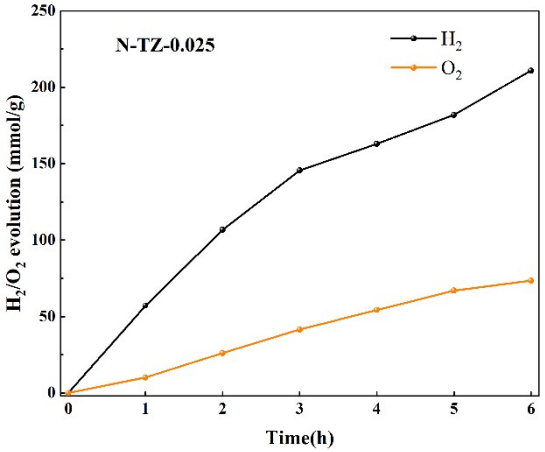

Figure S5. Photocatalytic H_2/O_2 evolution performance of N-TZ-0.025

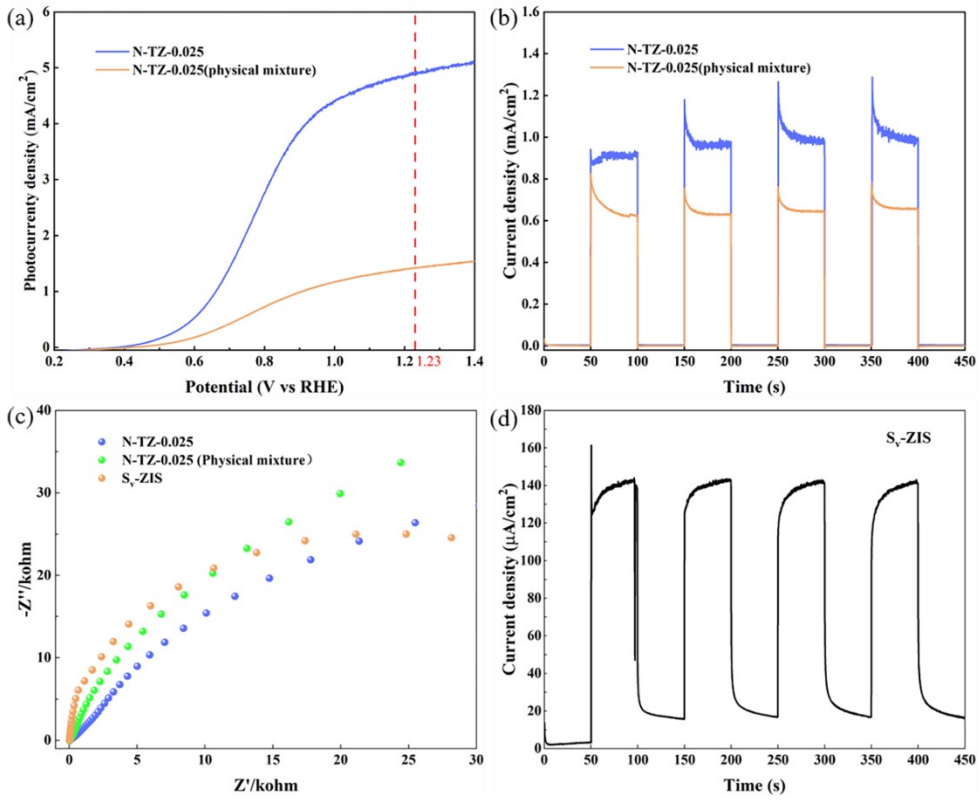

Figure S6. LSV curves (a) and photocurrent responses (b) of physically mixed N-TZ-0.025 and N-TZ-0.025 (a); (d) electrochemical impedance spectroscopy (EIS) of prepared samples; (d) photocurrent responses of pure Sv-ZIS.

As shown in Figure S6a and S6b, the photocurrent density of physically mixed N-TZ-0.025 reached 1.2 mA/cm^2 at the potential of 1.23V *vs.* RHE, which is much smaller than N-TZ-0.025. In Figure S6b, it is obvious to find that the physically mixed N-TZ-0.025 sample has a weaker photocurrent response than the N-TZ-0.025. In Figure S6c, the N-TZ-0.025 has a smaller arc radius, which indicates that the separation efficiency of electron-hole pairs is higher in the N-TZ-0.025 sample as the interface charge transfer is faster. Figure S6c implies the electrochemical measurements of pure Sv-ZIS, it can be seen the separation efficiency of electron-hole pairs is low and the interface charge transfer resistance is high. When coupled with the TiO_2 nanocone, the i-t activity and electrochemical properties of Sv-ZIS have noticeable improvements. Figure S6d shows the i-t activity of pure Sv-ZIS and the photocurrent density was ~140 μA/cm^2 under the same conditions as its counterpart samples, indicating the carrier recombination is severe.

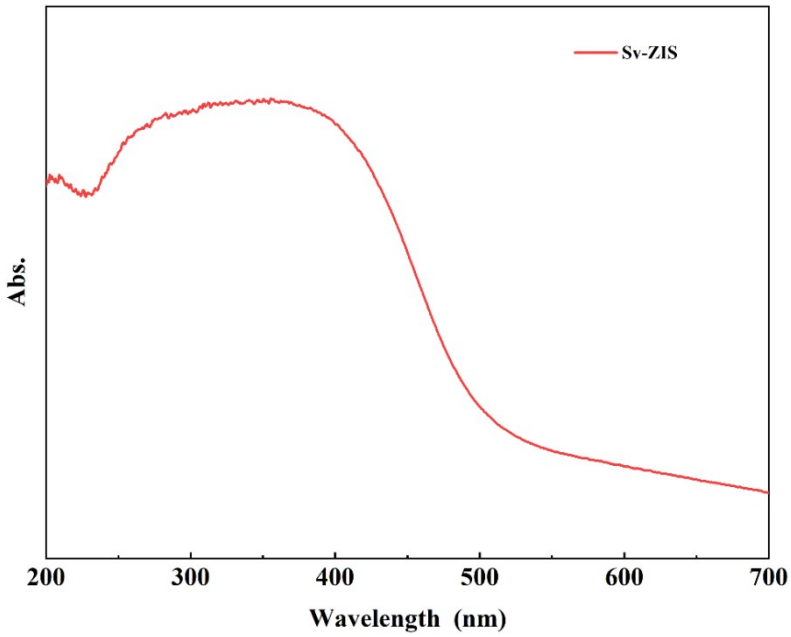

Figure S7 UV-vis absorption spectra of Sv-ZIS

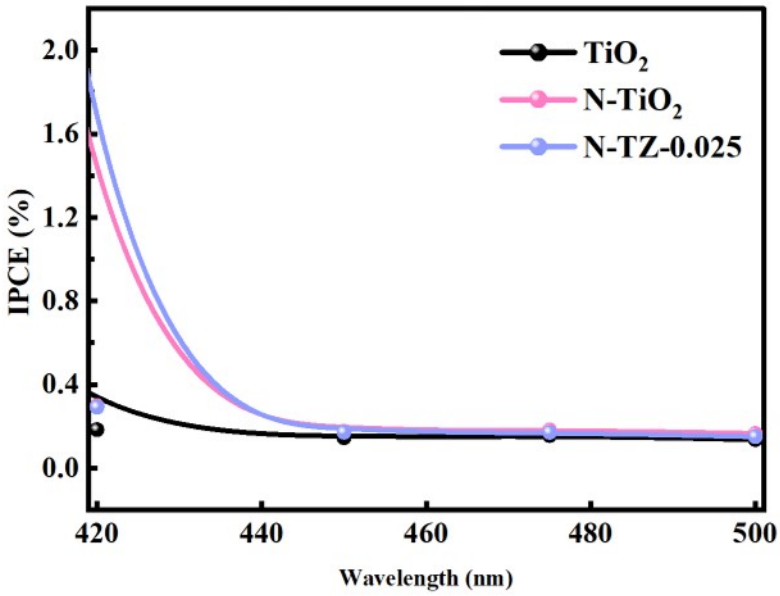

Figure S8 Measured IPCE in the visible-light range

Photoanode	**electrolyte**	**Photocurrent density** (at 1.23 V vs. RHE)	**IPCE**	**Ref.**
$ZnIn_2S_4/TiO_2$	0.35M Na_2SO_3 and 0.24M Na_2S	1.2 mA/cm^{-2}	21% at 380 nm	[1]
TiO_2/N-CDs	1.0 M NaOH	3.09 mA/cm^{-2}	65% at 390 nm	[2]
TiO_2-V_{Ti}/Fe_2O_3	1.0 M KOH	1.45 mA/cm^{-2}	29.8% at 340 nm	[3]
$TiO_2@Au_{25}/TiO_2$	0.5M Na_2SO_4	1.35 mA/cm^{-2}	45.2% at 318 nm	[4]
Au/N-TiO_2	1.0 M KOH	2.8 mA/cm^{-2}	60.7% at 300 nm	[5]
Y_2O_3/TiO_2	1.0 M KOH	0.609 mA/cm^{-2}	22% at 350 nm	[6]
PCN/Cu-TiO_2	0.2M Na_2SO_4	1.89 mA/cm^{-2}	31.2% at 415 nm	[7]
$TiO_2/BiVO_4$	0.2M Na_2SO_4	2.36mA/cm^{-2}	38% at 350 nm	[8]
$SrTiO_3/TiO_2$/Au	1.0 M NaOH	2.11 mA/cm^{-2}	59% at 340 nm	[9]
$CuInS_2/TiO_2$	0.5M Na_2SO_4	1.11 mA/cm^{-2}	57.7% at 400 nm	[10]
Sv-$ZnIn_2S_4$/N-TiO_2	0.5M Na_2SO_4	4.9 mA/cm^{-2}	57.9% at 350 nm	This work

Table S1 The representative IPCE results of TiO_2-based photocatalysts.

References

[1] Liu Q, Lu H, Shi Z, et al. 2D $ZnIn_2S_4$ Nanosheet/1D TiO_2 Nanorod Heterostructure Arrays for Improved Photoelectrochemical Water Splitting [J]. ACS Applied Materials & Interfaces, 2014, 6(19): 17200-7.

[2] Han Y, Wu J, Li Y, et al. Carbon dots enhance the interface electron transfer and photoelectrochemical kinetics in TiO_2 photoanode [M]. Applied Catalysis B: Environmental, 2022, 304: 120983.

[3] Li F, Jian J, Zou J, et al. Bulk embedding of Ti-defected TiO_2 nano-heterointerfaces in hematite photoanode for boosted photoelectrochemical water splitting [J]. Chemical Engineering Journal, 2023, 473: 145254

[4] Huo S, Wu Y, Zhao C, et al. Core-Shell TiO_2@Au25/TiO_2 Nanowire Arrays Photoanode for Efficient Photoelectrochemical Full Water Splitting [J]. Industrial & Engineering Chemistry Research, 2020, 59(32): 14224-33.

[5] Liang Z, Chen D, Xu S, et al. Synergistic promotion of photoelectrochemical water splitting efficiency of TiO_2 nanorod arrays by doping and surface modification [J]. Journal of Materials Chemistry C, 2021, 9(36): 12263-72.

[6] Sharma S, Shanmugam R, Harikrishna R B, et al. Y_2O_3 electrodeposited TiO_2 nanotube arrays as photoanode for enhanced photoelectrochemical water splitting [J]. International Journal of Hydrogen Energy, 2024, 52: 1415-27.

[7] Wang L, Si W, Ye Y, et al. Cu-ion-implanted and polymeric carbon nitride-decorated TiO_2 nanotube array for unassisted photoelectrochemical water splitting [M]. ACS Publications, 2021: 44184-44194.

[8] Guo Z, Wei J, Zhang B, et al. Construction and photoelectrocatalytic performance of $TiO_2/BiVO_4$ heterojunction modified with cobalt phosphate [M]. Journal of Alloys and Compounds, 2020, 821: 153225.

[9] Cheng X, Zhang Y, Bi Y. Spatial dual-electric fields for highly enhanced the solar water splitting of TiO_2 nanotube arrays [J]. Nano Energy, 2019, 57: 542-8.

[10] Han M, Wang Z, Zhang Z, et al. Rationally constructing intercrossed $CuInS_2$ nanosheets on TiO_2 nanorods for efficient photoelectrochemical water splitting [J]. Chemical Engineering Science, 2023, 281: 119151.